

# Effect of Environment on Mechanical Behavior of Thermosetting Composites Reinforced with Bio-filler (Orange Peel Particulate) Materials

Prajapati Naik <sup>1,2</sup>, Smitirupa Pradhan <sup>3</sup>, Prasanta Sahoo <sup>1,\*</sup> , Samir Kumar Acharya <sup>4</sup>

<sup>1</sup> Department of Mechanical Engineering, Jadavpur University, Kolkata, India

<sup>2</sup> Department of Mechanical Engineering, National Institute of Science and Technology, Berhampur, India

<sup>3</sup> School of Mechanical Engineering, KIIT Bhubaneswar, India

<sup>4</sup> Department of Mechanical Engineering, National Institute of Technology Rourkela, India

\* Correspondence: psjume@gmail.com; prasanta.sahoo@jadavpuruniversity.in (P.S.);

Scopus Author ID: 55562055400

Received: 9.06.2022; Accepted: 12.07.2022; Published: 11.09.2022

**Abstract:** The behavior of natural fiber depends upon different environmental conditions due to its hydrophilic nature. Therefore, this article has focused on the significant consequence of moisture absorption on the mechanical properties of bio-waste (orange peel) reinforced epoxy composites with different weight percentages (10%, 20%, and 30%) in different environmental conditions such as saline water treatment, steam treatment, and subzero temperature. After attaining saturation, the experiments were carried out by immersing the specimens in previously described environmental conditions—the percentage of moisture content in the fabricated composite increases with an increase in the filler loadings. The mechanical properties of environmentally affected composites were studied as per ASTM standards, and the same values were compared with the properties of the composite in normal environmental conditions. The cracked surface of the tested samples and morphology of orange peel particulates were analyzed by scanning electron microscope. X-ray diffraction and energy-dispersive spectroscopy (EDX) analysis also studied the characterization of orange peel particulates.

**Keywords:** bio-waste; orange peel; hydrophilic; saturation state; ASTM; SEM.

© 2022 by the authors. This article is an open-access article distributed under the terms and conditions of the Creative Commons Attribution (CC BY) license (<https://creativecommons.org/licenses/by/4.0/>).

## 1. Introduction

Worldwide, researchers focus on developing new composite materials, i.e., made up of natural fibers and eco-friendly waste materials. These composites can replace the most commonly used synthetic fibers for several purposes such as packaging, outdoor applications, automotive, etc. Natural fiber materials are more suitable due to their easy accessibility, eco-friendly, less expensive, high specific strength, and low density compared to non-biodegradable synthetic fibers. Due to the reasons mentioned above, the use of natural fiber, which acts as a reinforcing agent, in the composite industries has grown rapidly with the modification of some bottleneck properties [1-6]. The use of bio fiber in composite materials reduces the weight of the material by 10%, the cost of production by 5%, and the energy required for producing that material by 80% compared to synthetic fiber [7] in different sectors. However, due to the hydrophilic nature of bio fiber, they are not widely used in the polymer industries. Therefore, the study of bio-fiber in different weather conditions is crucial. The thickness, swelling behavior, and moisture absorption of bio-fiber reinforced composite

materials have many adverse effects on their performance and mechanical properties in long-term use [8-13]. The composite materials either release or absorb moisture completely depending upon environmental conditions [14, 15]. The moisture absorption in the bio-fiber composites is solely responsible due to the presence of hydroxyl groups in the natural fiber, forming hydrogen bonds within the fiber cell with water molecules [16-18]. The mechanism of moisture absorption by bio-fiber composite materials was well explained in several pieces of literature [19, 20].

The study of the influence of moisture absorption and thickness swelling of the bio-fiber reinforced composites is essential due to their applications in various industries. The moisture absorption behavior of polymer matrix composites was enhanced by adding rice husk particulate as reinforcement [21]. With filler loading increasing, the moisture content percentage increases due to more voids and celluloses [22]. They also reported that due to moisture absorption, the interfacial bonding between the matrix and reinforcement becomes weak; hence the mechanical properties deteriorate. Munoz and García-Manrique [23] observed that the mechanical properties of environmentally treated and raw flax fiber composite material increase due to the swelling behavior of fiber materials. Also, some researchers found that the moisture absorption and swelling thickness have less effect on the chemically treated composite mentioned above as compared to the untreated one [24].

The literature shows that very little research has been done considering orange peel particulate (OPP) as a filler material. Rathinavel and Saravanakumar [25] studied that the tensile property of treated polyvinyl and alcohol OPP enhanced significantly. Naik *et al.* [26] studied the erosive behavior of bio waste particulate reinforced epoxy composites for low-cost applications where OPP may be used as a filler material in composite industries. The filler content typically varies up to 30% for tribo-based applications [27]. However, the impact of different weight percentages of filler material in OPP composites on mechanical properties under different environmental conditions has not been noticed till now. Hence, a set of composites with different weight percentages OPP has been fabricated in this research work. The mechanical properties of composites under different weather conditions, such as steam, subzero temperature, and saline water, were studied according to ASTM standards. The thickness swelling behavior of different samples (raw and environmental affected) was also studied as per ASTM standards. The morphological analysis of environmentally treated and raw fabricated composites was studied by scanning electron microscope (SEM). This research has also done the surface morphology and surface chemistry of particulate by XRD and EDX analysis.

## 2. Materials and Methods

### 2.1. Materials.

Orange peels (OP) mainly contain cellulose, proteins, oils, and carbohydrates. For this reason, several researchers utilize this waste product for medicinal purposes. For this research analysis, OP was collected from the local market and cleaned carefully with distilled water to eliminate unwanted particles attached to the surfaces. After that, the OP was heated up to 100°C in an oven for 24 h to eliminate the water particles. The fibers were then ground into fine powder form with the help of a ball mill. The collected powders were sieved using a sieve shaker. The size of the particle used for this experiment is in the range of 1-212 µm. The chemical compositions and fixed carbon content, volatile matter, ash, and moisture content in

the OPP are explained by Naik *et al.* [27] while studying the abrasive wear behavior of OPP-reinforced composites. The different raw materials used in this research and their characteristics are presented in Table 1.

**Table 1.** Different raw materials used in the fabrication of composite.

Specimens	Characteristics
<b>Epoxy resin</b>	Grade:LY556 Chemical name: Diglycidyl-Ether of Bisphenol-A (DGEBA) Density: 1.1-1.2 (g/cm <sup>3</sup> ) Viscosity:10000-12000 (mPa-s)
<b>Hardener</b>	Grade:HY951 Chemical name:2-amineethylethane-1,2-diamin
<b>OPP</b>	Type: Bio waste material Density: 0.83 g/cm <sup>3</sup>

The microstructure and chemical characterization, morphological characteristics, and crystallite size of raw and environmentally treated OPP can be studied by EDX, SEM, and XRD analysis. The detailed procedure is explained elsewhere [28].

## 2.2. Sample preparation.

The composite specimens for the experimental observation were made by hand layup using a wooden mold with dimensions 160 mm×60 mm×6 mm. The samples were easily removed from the wooden mold by using the mold-releasing spray (heavy-duty silicone spray) at the interior part of the mold sheet. A required proportion, i.e., 10:1 by weight of epoxy and hardener, was properly mixed in a container and kept in a vacuum chamber to eliminate the air bubbles which were present in the mixture. Subsequently, the required amount of OPP was added to the mixture and mixed properly to attain different weight percentages of prescribed composites. Subsequently, the mixture was poured into the mold. The load was applied to the upper part of the mold, and it was allowed to cure under atmospheric conditions for 48 h. Due to applied load, some amount of mixture may be enfolded out from the mold. However, the maximum level of care was taken to maintain uniform thickness. The specimens were pulled out from the mold after the given time period. Subsequently, the specimens were cut into different sizes per ASTM standards for analysis of mechanical properties.

## 2.3. Mechanical testing.

A universal testing machine (UTM; H10KS, Hounsfield Test Equipment Ltd, England) is used for the tensile and flexural tests which were carried out according to ASTM D 3039–76 and ASTM D 790–03 standards, respectively. The UTM and test samples for tensile and flexural tests are shown in Figure 1. The crosshead speed was kept at 2 mm/min during the experiment for both tensile and flexural tests. Five specimens of each type were taken for observation, and the average value was taken for analysis. The flexural strength of different samples was evaluated using Eq.1.

$$\sigma = \frac{3FL}{2bt^2} \quad (1)$$

where F is the applied load at the breaking point, L is the span length, and b and t are the width and thickness, respectively.

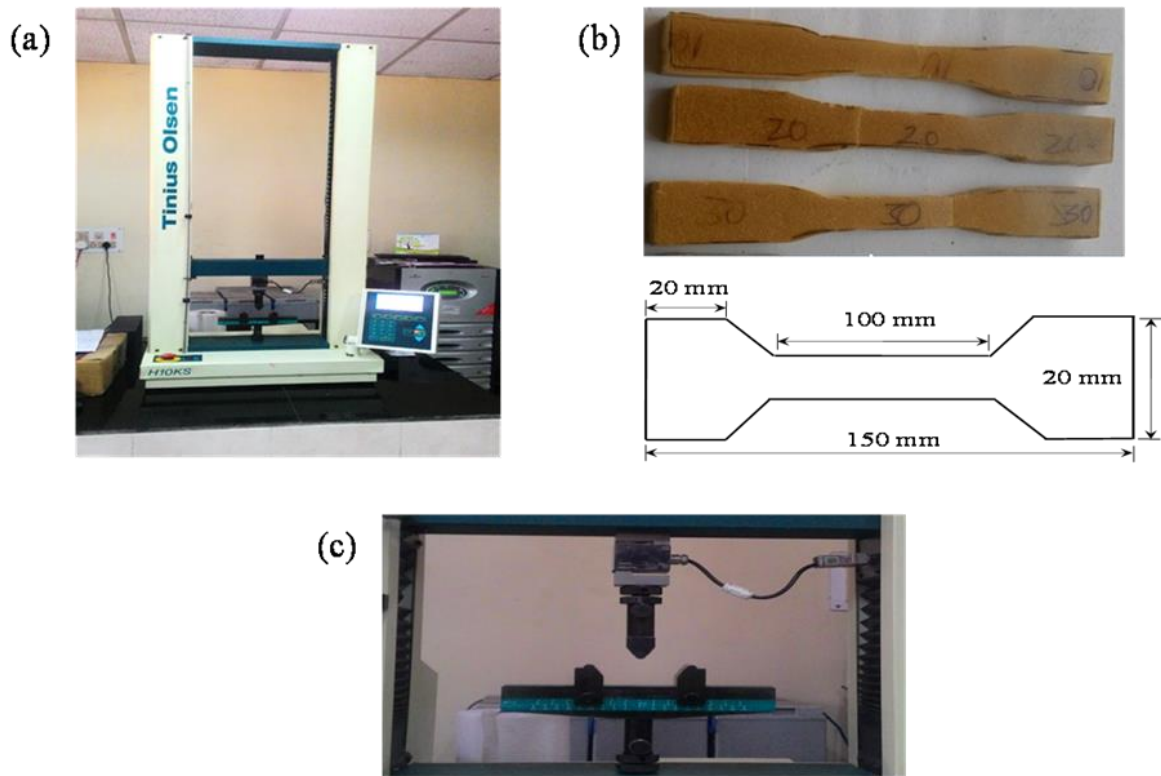


**Figure 1.** (a) Hounsfield H10 KS UTM; (b) Sample for the tensile test; (c) Arrangement for the flexural test (Three-point bend test).

#### 2.4. Moisture absorption and thickness swelling test.

The thickness swelling behavior and moisture absorption of the different test specimens were evaluated as per ASTM D 570-98 standard. The test specimens were heated in an oven at 100° C to remove the moisture and cool to the ambient temperature in a desiccator containing silica gel. The weight of the test sample was measured before immersing it in different environmental conditions, such as saline water (5% NaCl), steam treatment, and subzero temperature (-25°C). The specimen was then removed after 12 h exposure, and the moisture was removed with the help of tissue paper or a dry clean cloth. Sufficient care was taken to eliminate all the moisture from the specimen. Then the weight of the samples was measured again by an electronic weight machine with a reading capacity of  $\pm 0.1 \text{ mg}$  within one minute of removal from the environmental chamber. The observations were carried out for 72 h, and the weight was measured regularly within 12 h. The percentage of moisture absorption of samples was estimated using the weight difference between the environmentally treated and untreated samples as given in Eq. 2.

$$\Delta M(t) = \frac{M_t - M_0}{M_0} \quad (2)$$

where  $\Delta M(t)$  is the % of weight gain in the samples due to moisture content.  $M_t$  and  $M_0$  are the weight of treated and untreated specimens, respectively. Five specimens of each set were taken for observation, and the average and standard deviation data were reported from the observation. A similar procedure was also followed to work out the thickness swelling behavior of the fabricated specimen using Eq. 3.

$$\Delta T = \frac{T_t - T_0}{T_0} \quad (3)$$

where  $T_t$  and  $T_0$  are the thickness of environmentally affected and dry samples, respectively. When the sample's weight change is less than 0.01%, it is assumed that the sample will reach an equilibrium state.

### 3. Results and Discussions

#### 3.1. EDX analysis.

The EDX analysis represents the peaks for different materials according to their binding energies. It is observed that the shape and size of particles in OPP vary, and they are mainly in fibrous, spherical, and prismatic forms. The prismatic particles generally contain Si and O, whereas the spherical particulates contain O and Si along with Ca and Al. From EDX analysis, it has been observed that the percentage of calcium, aluminum, and silicon is very less in comparison to C. Carbon is the fibrous material presented in the OPP. The percentage of carbon and oxygen present in OPP in different environmental conditions is shown in Table 2, where it is noticed that mainly carbon and oxygen are present in the OPP, and a very less amount of Si, Ca, Cl, Na, and K are present which are not mentioned here. It is also observed that the percentage of carbon compound decreases when it is exposed to different environmental conditions. A minimum reduction of the percentage of carbon content is seen in a saline environment, whereas the maximum reduction of percentage is in steam treatment. The EDX analyses of environmentally treated OPP Composite materials are shown in Figure 2.

**Table 2.** EDX analysis of OPP.

Environmental conditions	% C	% O
Normal sample	73.91	17.56
Saline water	55.80	24.81
Steam Water	50.37	48.25
Subzero Temp	52.85	44.93

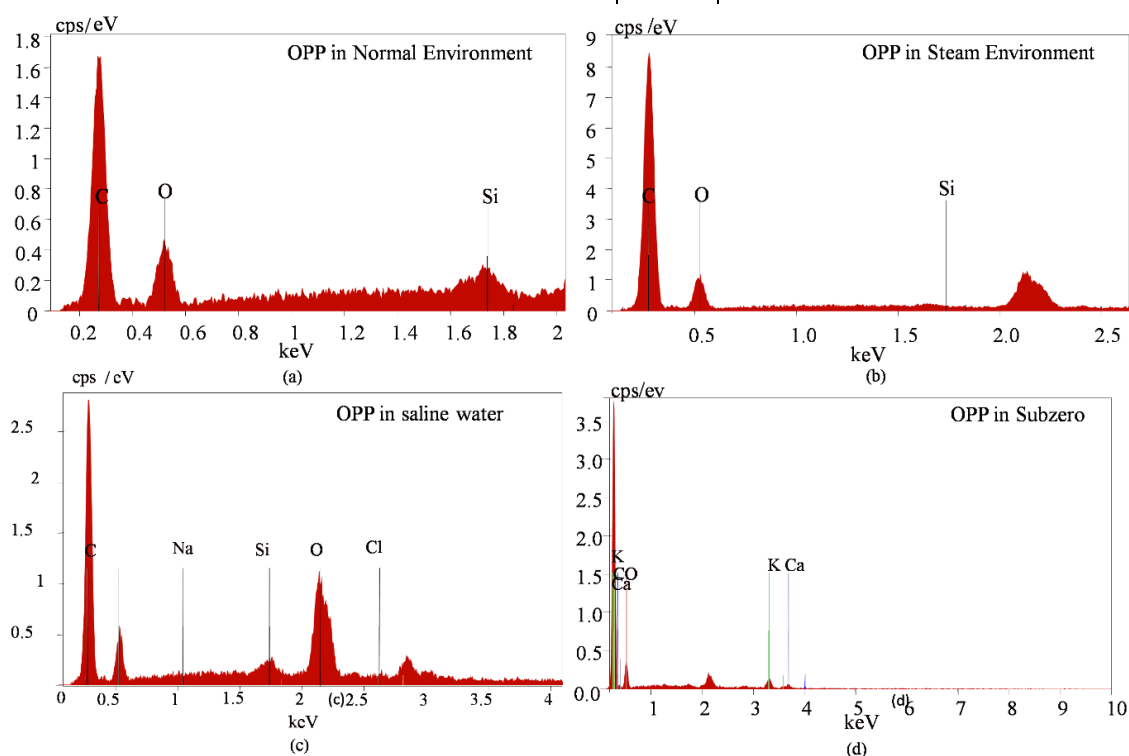


**Figure 2.** EDX analysis: (a) Normal environment, (b) Steam environment, (c) Saline water environment, and (d) Subzero environment.

### 3.2. XRD analysis.

XRD analysis was used for analyzing the crystallographic structure of materials. An X-ray diffractometer with graphite monochromameter with a voltage 40 mV and a current of 40 mA was used for the analysis. The diffraction intensity at an angle  $2\theta$  is between  $10^\circ$  to  $45^\circ$ . XRD analysis of the OPP samples is represented in Figure 3. It has been evaluated that the observed samples contain a large number of noises, which explains the amorphous nature of carbon. The crystalline peak in each profile occurred at around  $22.7^\circ$  at an angle of  $2\theta$ . From Figure 4, it is observed that the peaks are found at  $12.23^\circ$ ,  $22.7^\circ$ ,  $34.5^\circ$ , and  $42.3^\circ$  which shows the crystalline nature of the carbon, and the remaining is the amorphous nature of the natural fiber. The amorphous nature shows the existence of lignin and hemicelluloses in the OPP. The materials' crystalline index ( $I_c$ ) is calculated using Eq. 4.

$$I_c = \frac{I_{002} - I_{am}}{I_{002}} \quad (4)$$

where  $I_{002}$  is the lattice peak for the maximum intensity diffraction (002) at an angle of  $2\theta$  between  $22^\circ$  and  $23^\circ$ ,  $I_{am}$  is the minimum diffraction intensity of the amorphous material at an angle of  $2\theta$  between  $15^\circ$  and  $16^\circ$ .

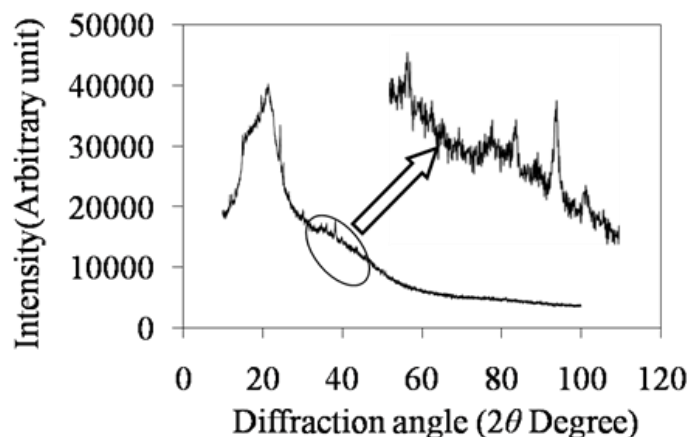
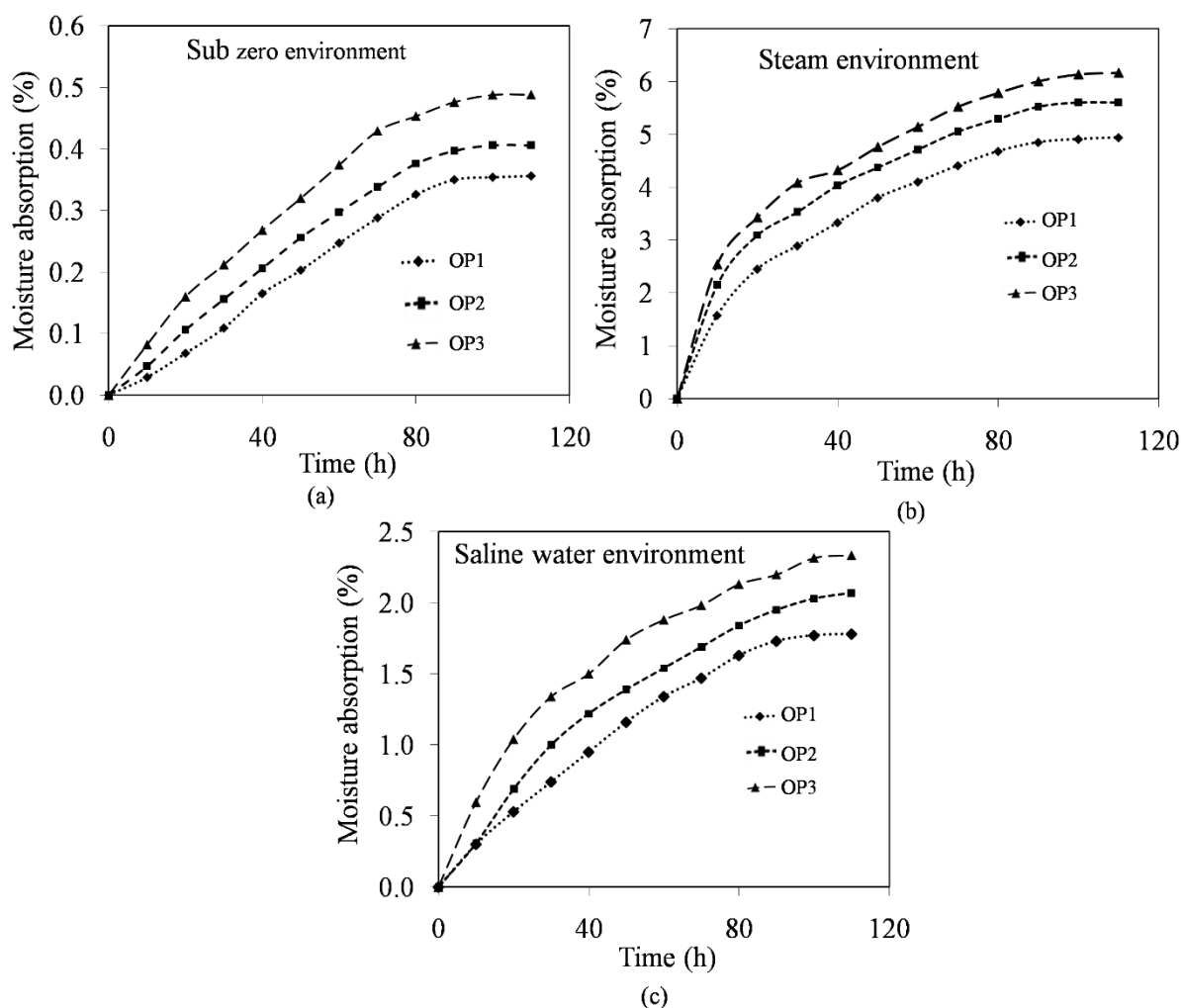


Figure 3. XRD analysis of OPP.

### 3.3. Moisture absorption

The water absorption trends of different specimens, such as OP1, OP2, and OP3 (10%, 20%, and 30%, respectively), exposed to different environmental conditions such as subzero temperature, steam, and saline water, are shown in Figure 4. It is noticed that the weight of the sample increased when it was treated in all environmental conditions, irrespective of the weight percentage of filler materials. This may be due to the moisture absorption of the specimens, and the maximum moisture intake was noticed in the case of OP3 composite. This is mainly due to the presence of porosity and the lumen. The moisture intake is also due to the matrix and fiber adhesive nature [28]. However, the presence of voids is mostly responsible for the hydrophilic nature of the OPP and weak adhesion bonding between particulate and matrix. The number of free  $-OH$  groups of cellulose of OP rises with an increase in the percentage of particulates in the composite due to moisture absorption. The free  $-OH$  groups of natural fiber come in contact with water molecules to form hydrogen bonds. Due to the above reason, there is an increase in weight in the samples after exposure to different treatments, and consequential outcomes of the natural fiber after moisture absorption are shown in Figure 5.





**Figure 4.** Moisture absorption behavior of OPP composites: (a) Sub zero environment; (b) Steam environment; (c) Saline water environment.

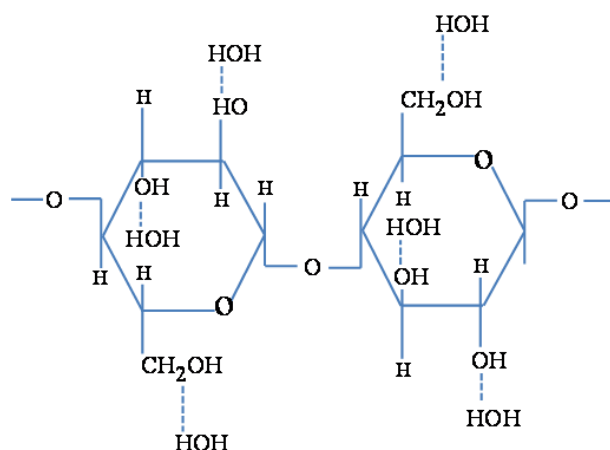


**Figure 5.** Schematic diagram of the natural fiber after moisture absorption.

The maximum moisture absorption (MMA) of developed composites under different environmental conditions is presented in Figure 6. It is noticed that the MMA value increases with the increase of the filler loadings, and the OP3 composite shows the maximum value. It is also observed that the moisture absorption rate is higher in the case of steam water than in the saline environment for all the filler loadings. The deposition of NaCl ions is there on the surface of the composite specimens when it is put in the saline water. And it increases with the increase of immersion time, which reduces the rate of water diffusion. The MMA value is much

less in subzero treatment because of low intermolecular hydrogen bonding compared to other environmental treatments. Similar behavior was observed by Raghabendra *et al.*[29] while studying jute epoxy composites.

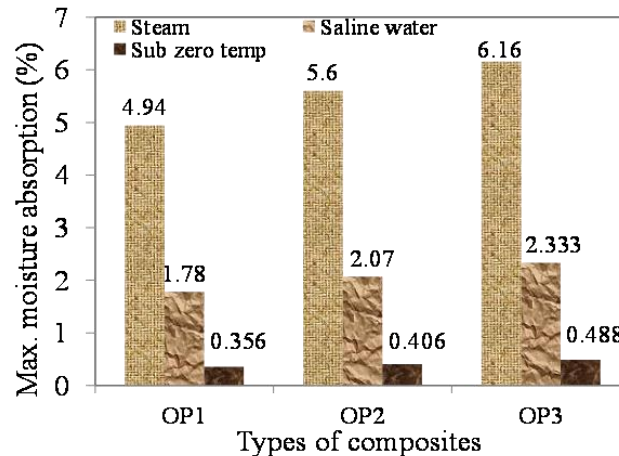


**Figure 6.** Maximum moisture absorption of OPP composites in different environments.

### 3.4. Diffusivity and kinetics of moisture absorption.

According to the Fickian diffusion process, the rate of moisture absorption in the different composite is quite high at the initial phase when they are exposed to different environments; after that, the rate of absorption is decreased and reached to almost saturation stage, as shown in Fig. 7. This can be explained clearly by taking the moisture absorption properties of the OPP. When the specimens are exposed to different environments, the swelling of the sample starts due to the water intake quality of natural fiber. As a result, micro-cracking occurs in the specimens. The cracks in the sample are responsible for capillarity action, and due to the presence of micro-cracks, the transfer of water molecules is possible. The times required to attain the saturation stage for different samples are not the same when they are exposed to different environments. It is noticed that the saturation time for steam, saline water, and subzero temperature is 60, 70, and 30 h, respectively.

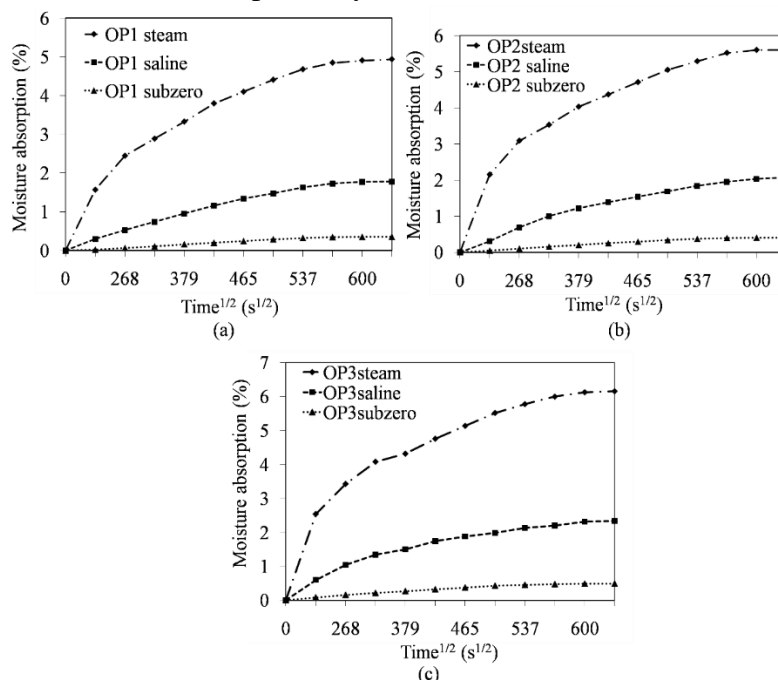


**Figure 7.** Moisture absorption of different weight percentage: (a) OP1; (b) OP2; (c) OP3 in different environments.



The rate of moisture absorption is maximum for 30 wt% particulate reinforced composite under steam environmental conditions and minimum for subzero conditions, as shown in Fig. 8. Higher temperature (steam environmental condition) seems to pick up the pace of water absorption quality. The moisture absorption rate is less in saline water compared to steam; this may be due to the deposition of NaCl ions on the surface of the specimen as described previously and subsequently creates obstructs for water diffusion. Again, the percentage of water absorption in subzero temperature is lowest compared to other environments due to a decrease in intermolecular hydrogen bonding. Fick's theory analyzed the diffusion mechanism and kinetics and fit the experimental values.

$$\log \left( \frac{M_t}{M_m} \right) = \log(k) + n \log(t) \quad (5)$$

where  $M_t$  and  $M_m$  are the moisture absorption at time  $t$  and saturation stage.  $k$  and  $n$  are constants. The fitting parameters from the observation data for OPP composite under a steam environment are shown in Fig. 8. Similarly, the values of  $n$  and  $k$  are found from the curve fitting for other environmental conditions and are given in Table 3.

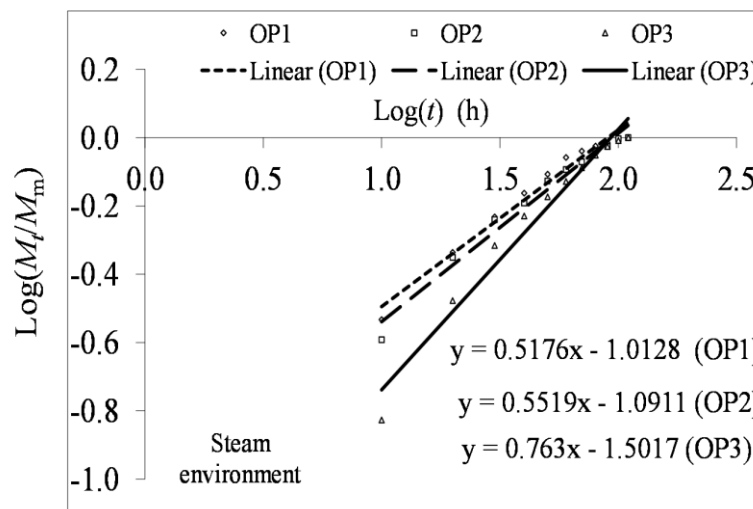


**Figure 8.** Diffusion curve fitting for OPP composite in Steam treatment.

**Table 3.** Fitting parameters ( $n$ ,  $k$ , and  $h$ ) for different filler loading for all environmental conditions.

Environment	Filler Loading (%)	$n$	$k$	Diffusivity ( $D_x$ ) ( $\text{mm}^2/\text{s}$ )
Steam	OP1	0.5176	0.097	$3.32 \times 10^{-5}$
	OP2	0.552	0.081	$5.72 \times 10^{-5}$
	OP3	0.763	0.031	$3.46 \times 10^{-5}$
Saline	OP1	0.374	0.179	$2.1 \times 10^{-5}$
	OP2	0.403	0.160	$2.64 \times 10^{-5}$
	OP3	0.481	0.113	$4.77 \times 10^{-5}$
Subzero	OP1	0.671	0.048	$3.46 \times 10^{-5}$
	OP2	0.759	0.032	$3.55 \times 10^{-5}$
	OP3	0.911	0.016	$2.09 \times 10^{-5}$

Diffusion coefficient (diffusivity) ( $D_x$ ) is used to evaluate the amount of moisture absorbed by the composite samples. The diffusivity has a significant impact on Fick's model. Figure 8 shows the percentage of moisture absorption ( $M_t$ ) versus the square root of time, and the relationship between moisture absorption and time is presented in Eq. 6.

$$\frac{M_t}{M_m} = \frac{4}{\sqrt{\pi}} \sqrt{\frac{t D_x}{h^2}} \quad (6)$$

where  $h$  represents the thickness of the sample. The diffusivity ( $D_x$ ) can be evaluated by using Eq. 7.

$$D_x = \pi \left[ \frac{h}{4M_m} \right]^2 \left[ \frac{M_2 - M_1}{\sqrt{t_2} - \sqrt{t_1}} \right]^2 \quad (7)$$

where  $t_1$  and  $t_2$  are preferred time periods in the initial linear portion.  $M_1$  and  $M_2$  are the amounts of moisture contents at times  $t_1$  and  $t_2$ , respectively. It is observed that the diffusivity and corresponding maximum moisture content of the fabricated composite specimens improves steadily with an increase in filler loading in all environments, as shown in Table 4. The increase rate is higher in specimens exposed to steam than those subjected to other environmental conditions. The samples containing more wt% filler material confirm better diffusivity in all environments due to the higher amount of cellulose content.

### 3.5. Thickness swelling behavior.

Generally, the composite swells due to moistures present in different environmental conditions. The swelling thickness ( $\Delta T$ ) and swelling rate parameter (KSR) for different OPP composites in the prescribed environments have been evaluated. A nonlinear regression curve fitting technique was used to fit the experimental data in Eq. 7 to evaluate the  $\Delta T$  and KSR. The curve fitting approach is used to analyze the thickness swelling behavior [30].

$$\Delta T = \left[ \frac{H_\infty}{H_o + (H_\infty - H_o)e^{-K_{SR}t}} - 1 \right] \quad (8)$$

where  $H_0$  and  $H_\infty$  are the thickness of the developed composite material at initial and equilibrium conditions. The KSR value obtained from the nonlinear curve fitting diagram is presented in Table 4. It has been observed that the KSR value increases with filler loadings, and the maximum value is observed in the case of OP3 composites in a steam environment (Table 4). This might be due to more microvoids in the higher wt % filler specimens. Hence, there is weak interfacial adhesion bonding between filler (hydrophilic OPP) and matrix materials (hydrophobic epoxy). It is also observed that the higher KSR value signifies a higher rate of swelling along with reaching equilibrium within a very short span of time. Several researchers also found similar types of results [31, 32]. The variation of thickness with different wt% is reported in Figure 10. The thickness swelling behavior of the specimen increases with an increase in the filler loadings. However, it is different for different environmental conditions. Due to the presence of cellulose, the OPP materials contain a free  $-OH$  group; hence, they absorb moisture easily when exposed to different environments.

**Table 4.** KSR of OPP composite in different environments.

Environment	Filler Loading (%)	$H_o$	$H_\infty$	$\Delta T$ (%)	$K_{SR} \times 10^{-3} (h^{-1})$
Steam	OP1	6.833	6.911	1.136	49.9
	OP2	5.663	5.733	1.230	44.2
	OP3	7.060	6.169	1.360	51.8
Saline	OP1	6.607	6.673	0.994	45.1
	OP2	5.573	5.620	0.840	44.6
	OP3	6.917	6.969	0.753	50.4
	OP1	5.640	5.769	2.290	36.0

Environment	Filler Loading (%)	$H_o$	$H_{\infty}$	$\Delta T$ (%)	$K_{SR} \times 10^{-3} (h^{-1})$
Subzero	OP2	5.450	5.563	2.072	35.7
	OP3	6.900	7.022	1.770	41.5

The moisture content in OPP composite (filler) increases in the steam environment (as shown in Figure 7) due to its hydrophilic nature and micropores on the surface. The presence of microvoids is responsible for a weak bond between the matrix (hydrophobic) and filler (hydrophilic) material [33, 34]. It is also observed that the swelling tendency of fabricated samples in a steam environment is higher than in other environments. The maximum thickness swelling (MTS) was observed in the fabricated OP3 composite containing (as shown in Figure 9) irrespective of the environmental conditions. The MTS values are 2.29%, 2.072%, and 1.77% for steam, saline water, and subzero temperature, respectively (Figure 9d). A similar type of behavior was also observed by Haameem *et al.* [35] for Napier grass composites.

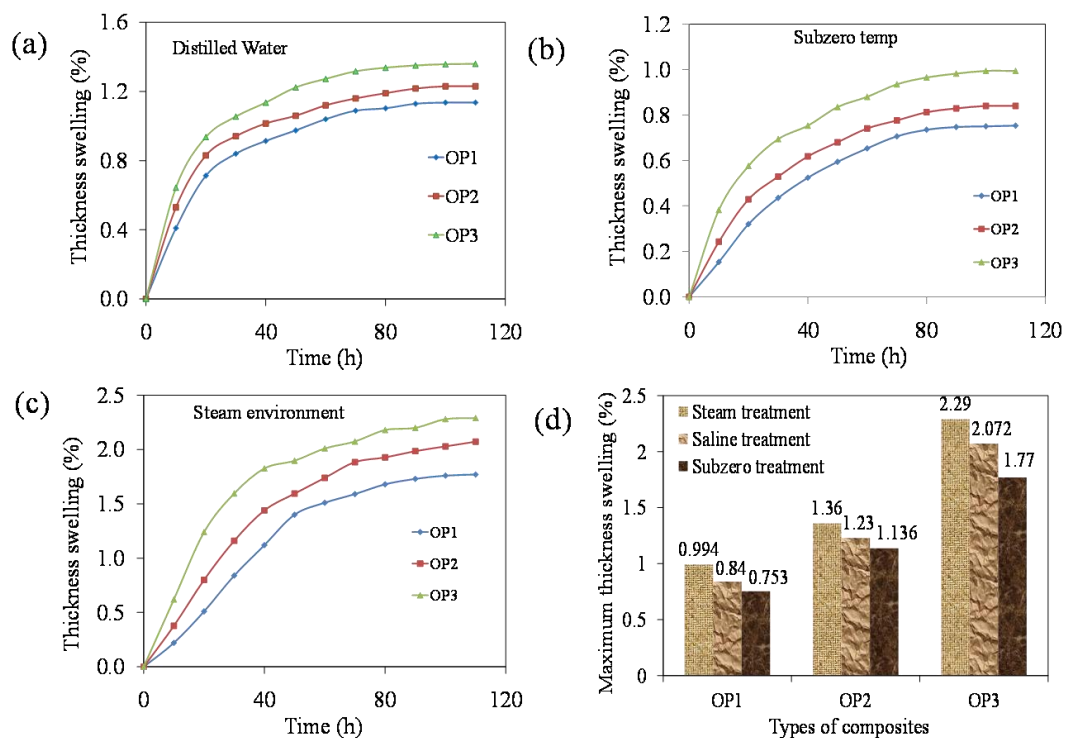


**Figure 9.** Thickness swelling behavior of different composites: (a) Saline water treatment; (b) Subzero temperature; (c) Steam temperature environment; (d) Maximum thickness swelling (MTS) of OPP composite at different environmental conditions.

### 3.6. Effect of moisture absorption on mechanical properties.

After exposure to ambient temperature and different environmental conditions, the effect of mechanical properties, i.e., flexural strength and tensile strength of different wt% of the OPP reinforced epoxy composites, are shown in Figure 10. Initially, with an increase in filler loading (wt% up to 20%), the tensile strength of the fabricated material increases; subsequently, it reduces (i.e., OP3 composite) (as shown in Figure 10a). Patel *et al.* also noticed a similar moisture absorption behavior [36] while studying the environmental effect of water absorption and the flexural strength of red mud-filled jute/fiber/polymer composites. At higher wt% of filler loading, the epoxy quantity is insufficient to saturate the filler material, affecting the reinforcement's wet ability. Hence, the strength of adhesion bonding between matrix and reinforcement decreases. The strength of the fabricated specimens with higher wt% (OP3)

deteriorates as sufficient load transfer is not possible from the matrix to fiber. The effect of filler loadings on the flexural strength of treated (in different environments) and untreated composites is presented in Figure 10b. The flexural strength increases with an increase in the wt% of particulate (amount of OPP up to 20%) in the case of untreated (normal atmospheric conditions) specimens. The reason is due to the quality of reinforcement which resists bending force and more load transfer from the matrix [37, 38]. It is noticed that the flexural strength of OPP composite decreases when they are exposed to different environments, as shown in Figure 10b. Exposure of specimens to different environmental conditions affects interfacial adhesion between matrix and fiber, which is responsible for debonding and decreases flexural strength [35].

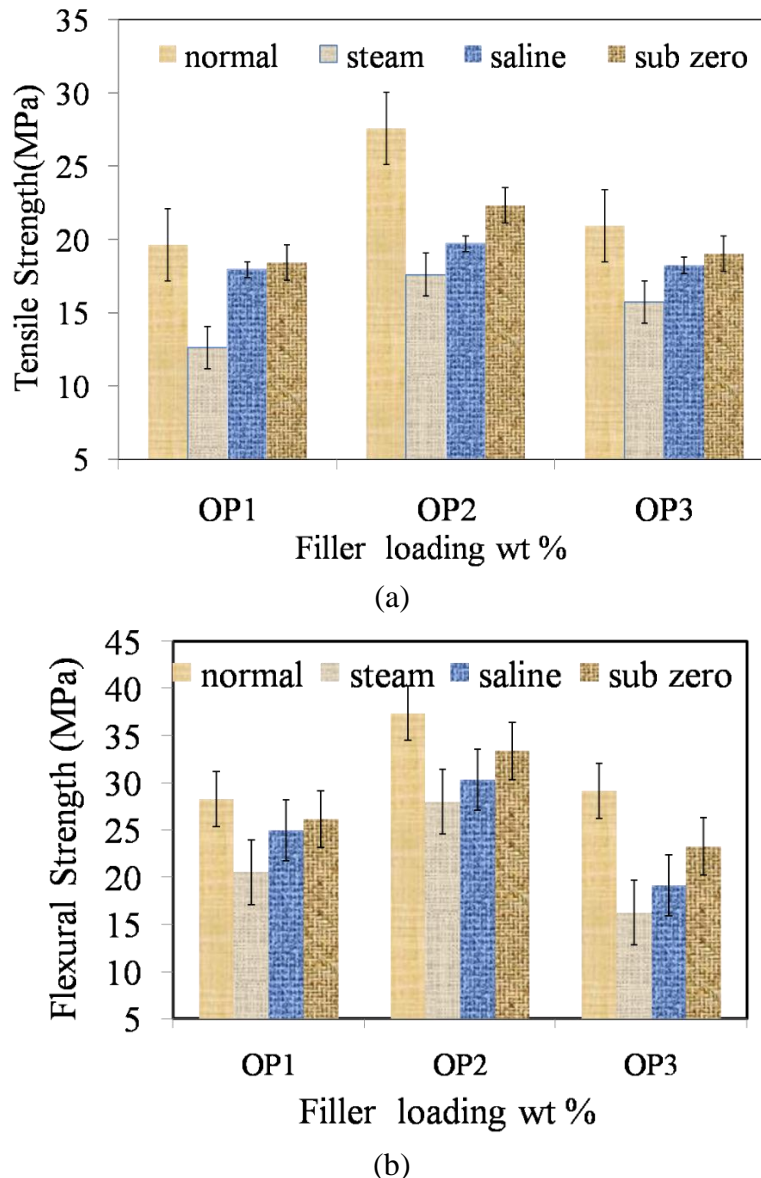


**Figure 10.** Effect of incorporation of different wt% of OPP filler on mechanical properties and its consequence when treated in different environments: **(a)** Tensile strength; **(b)** Flexural strength.

Moisture is absorbed in the polymer either in the form of bound water or free water [39]. The water molecules which are spread over a wide range in a polymer matrix, attracted towards the polar groups of the polymer, are known as bound water, and the water molecules which move freely through microvoids and pores are known as free water [40]. When the specimens are exposed to different environments, the water molecules are attached to the natural fiber composite micro-cracks and decrease the interfacial adhesion between fiber and

matrix. This is the cause for the swelling of specimens and development of micro-cracks in the matrix, and in due course of time, there is the chance of debonding between matrix and filler material. The moisture absorption and thickness swelling have a significant role in the mechanical properties of bio composite materials. Figure 10 shows that the environmentally treated bio composite specimens follow similar tensile and flexural behavior as in the untreated case. However, it is observed that biowaste-reinforced material's mechanical strength is reduced when exposed to different environments. This property reduction is due to transformation in the fiber/matrix interface and the fiber observed from SEM analysis. When the interface of fiber/ matrix is exposed to a different environment, the cellulosic (natural) material tends to swell, which results in the progress of shear stress at the surface interface. This is the reason for reducing the strength of the specimen due to debonding of fiber and matrix. The above analysis shows that the fiber loading and the exposure of specimens to different environments have significant roles in their mechanical properties. The maximum reduction in the strength was observed in the steam environment, and the minimum reduction in the case of the subzero temperature condition. This is due to the less moisture absorption in the case of the subzero environment, as discussed in the previous section. Many authors also observed similar behavior [29, 34, 39].

### 3.7. Surface morphology.

The surface morphology of the OPP materials was observed by the SEM approach, and it is presented in Figure 11. It is observed that the OPP surface is denser and more planner. Some porous structures are visible at higher magnification. The fractography of raw and OP2 composite specimens exposed in steam water is shown in Figure12, obtained from SEM after the tensile and flexural test. After the mechanical test of the fabricated samples, matrix filler debonding, pull out of filler materials, and matrix fracture fiber breakage can be observed through SEM.

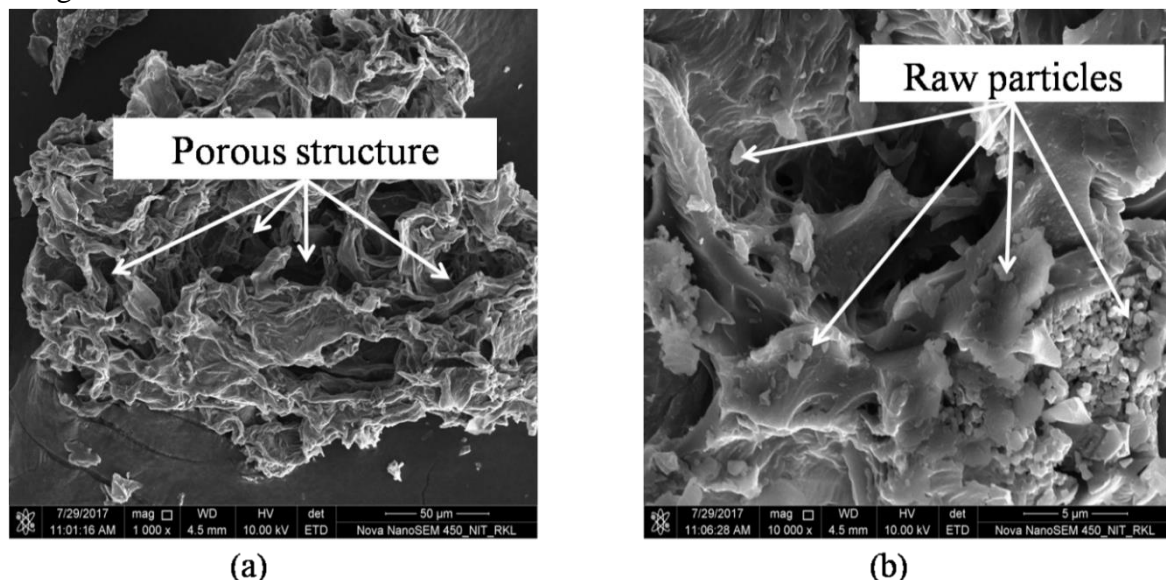


**Figure 11.** SEM morphology of OPP at different locations.

The surface morphology of raw OP2 composites after the tensile test is shown in Figure 12a. It is clearly observed that the debonding between matrix and filler material occurs due to poor compatibility between matrix and filler material. Although, there is no sign of pulling out filler materials from the matrix resin. The surface morphology of steam water-treated OP2



composites under tensile load is presented in Figure 12b. Fiber matrix debonding is observed from the SEM analysis. Due to fiber swelling, there is a visible pull-out of filler material from the specimens and matrix filler debonding. This might be due to the presence of voids responsible for water passage in the composite specimens, which leads to the swelling of composite specimens to crack the composite materials.

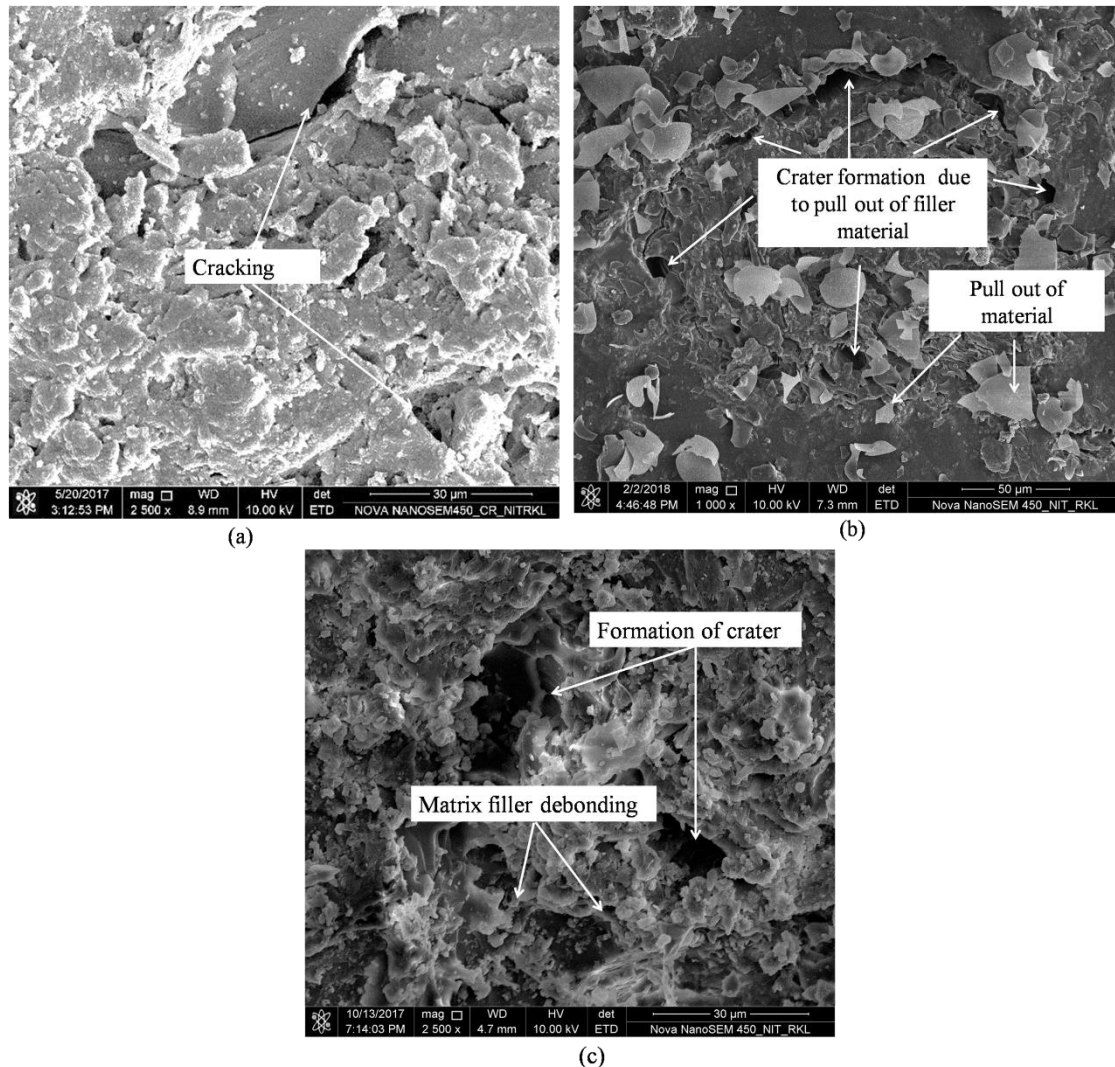


**Figure 12.** SEM morphology (a) Raw OP2 composites after tensile test; (b) OP2 with steam water treatment after tensile test; (c) OP2 steam water treatment after the flexural test.

The surface morphology of OP2 composite exposed to steam treatment after a flexural load test is shown in Figure 12c. The matrix cracking and fiber breakage is visible from the SEM analysis. This is due to swelling of filler material and poor compatibility between filler and matrix material. Due to the swelling of filler material, micro-cracks are formed at the interface of the composite specimen. These micro-cracks are responsible for moisture absorption in the fiber matrix interface region. Therefore, the matrix fiber debonding and pulling out of filler material is visible at higher magnification.

The present study considers OPP as a bio-filler in the composite to evaluate the effect of the environment in terms of moisture intake and thickness swelling behavior. To improve the durability of the composite, one needs to adopt methods to avoid such degradation. In this respect, researchers typically look for different surface coating techniques, including electroless nickel deposition [41-46], where a thin nickel-based coating helps prevent moisture absorption and subsequent degradation of the composite. Apart from this, OPP can be given



pre-treatment [47] or converted to natural carbon black [48] before using it as filler material in the composite. Also, similar studies on environmental degradation can be attempted in the future using other bio-waste materials like clamshell [49], eggshell [50], crab shell [51], etc.

#### 4. Conclusions

In the present research, the water intake quality and thickness swelling of developed composite samples have been studied, and their consequences on mechanical properties have been studied. The subsequent results are listed below: It is observed that the moisture intake and thickness swelling behavior of fabricated samples increases with increasing the percentage of OPP filler material for different environmental conditions; The environmental conditions have a significant role in the moisture absorption and swelling behavior of different OPP composites. The developed OPP composites subjected to a subzero environment absorb less moisture in comparison to other environmental conditions. The composites exposed to a steam environment absorb maximum moisture; The moisture absorption pattern follows the Fickian diffusion behavior in all environmental conditions. The diffusion coefficient value is more prominent in the steam water environment and less in the subzero environment; The thickness swelling behavior of OPP composite increases with increasing the filler loadings. The  $K_{SR}$  of the fabricated composite specimens increases with an increase in the filler loadings for all environmental conditions. OP3-based composite material indicates the highest thickness swelling rate. The values of  $K_{SR}$  are higher in the case of the steam environment, followed by saline and subzero environments; The mechanical properties of developed composites after exposing different environmental conditions decrease as compared to the same sample of the same weight percentage under normal environmental conditions. In a steam water environment, there is maximum degradation of mechanical properties. However, the minimum degradation is observed in the case of a subzero environment; From the SEM analysis, it is concluded that the failure of environmentally treated OPP composites is due to the swelling of filler material that caused the debonding between filler and matrix.

#### Funding

This research received no external funding.

#### Acknowledgments

None.

#### Conflicts of Interest

The authors declare no conflict of interest.

#### References

1. Faruk, O.; Bledzki, A. K.; Fink, H. P.; Sain, M. Biocomposites reinforced with natural fibers 2000-2010. *Progress in Polymer Science* **2012**, *37*, 1552-1596, <https://doi.org/10.1016/j.progpolymsci.2012.04.003>.
2. Mohanty, A. K., Khan, M.A.; Hinrichsen, G. Surface modification of jute and its influence on performance of biodegradable jute-fabric/Biopol composites. *Composites Science and Technology* **2000**, *60*, 1115-1124, [https://doi.org/10.1016/S0266-3538\(00\)00012-9](https://doi.org/10.1016/S0266-3538(00)00012-9)

3. Gassan, J.; Bledzki, A. K. Possibilities for improving the mechanical properties of jute/epoxy composites by alkali treatment of fibres. *Composites Science and Technology* **2000**, *59*, 1303-1309, [https://doi.org/10.1016/S0266-3538\(98\)00169-9](https://doi.org/10.1016/S0266-3538(98)00169-9).
4. Geethamma, V. G.; Mathew, K. T.; Lakshminarayanan, R.; Thomas, S. Composite of short coir fibres and natural rubber: effect of chemical modification, loading and orientation of fibre. *Polymer* **1998**, *39*, 1483-1491. [https://doi.org/10.1016/S0032-3861\(97\)00422-9](https://doi.org/10.1016/S0032-3861(97)00422-9).
5. Sharifah, H. A.; Martin, P. A. The effect of alkalization and fiber alignment on mechanical and thermal properties of Kenaf and Hemp bast fiber composite. Part-I Polyester resin matrix. *Compos Sci Technol* **2004**, *64*, 1219–1230, <https://doi.org/10.1016/j.compscitech.2003.10.001>
6. Alawar, A.; Hamed, A. M.; Al-Kaabi, K. Characterization of treated date palm tree fiber as composite reinforcement. *Composites Part B: Engineering* **2009**, *40*, 601-606, <https://doi.org/10.1016/j.compositesb.2009.04.018>.
7. Mohammed, L.; Ansari, M. N.; Pua, G.; Jawaidd, M.; Islam, M. S. A review on natural fiber reinforced polymer composite and its applications. *International Journal of Polymer Science* **2015**. <https://doi.org/10.1155/2015/243947>.
8. Ahmad, F.; Choi, H. S.; Park, M. K. A review: natural fiber composites selection in view of mechanical, light weight, and economic properties. *Macromolecular Materials and Engineering* **2015**, *300*, 10-24, <https://doi.org/10.1002/mame.201400089>.
9. Espert, A.; Vilaplana, F.; Karlsson, S. Comparison of water absorption in natural cellulosic fibres from wood and one-year crops in polypropylene composites and its influence on their mechanical properties. *Composites Part A: Applied Science and Manufacturing* **2004**, *35*, 1267-1276, <https://doi.org/10.1016/j.compositesa.2004.04.004>.
10. Al-Oqla, F. M.; Sapuan, S. M.; Ishak, M. R.; Nuraini, A. A. A novel evaluation tool for enhancing the selection of natural fibers for polymeric composites based on fiber moisture content criterion. *BioResources* **2015**, *10*, 299-312.
11. Wang, W.; Sain, M.; Cooper, P. A. Study of moisture absorption in natural fiber plastic composites. *Composites Science and Technology* **2006**, *66*(3-4), 379-386, <https://doi.org/10.1016/j.compscitech.2005.07.027>.
12. Tajvidi, M.; Ebrahimi, G. Water uptake and mechanical characteristics of natural filler–polypropylene composites. *Journal of Applied Polymer Science* **2003**, *88*, 941-946, <https://doi.org/10.1002/app.12029>.
13. Ramesh, M.; Palanikumar, K.; Reddy, K. H. Influence of fiber orientation and fiber content on properties of sisal-jute-glass fiber-reinforced polyester composites. *Journal of Applied Polymer Science* **2016**, *133*, <https://doi.org/10.1002/app.42968>.
14. Costa, M. L.; Almeida, S.F.M.D.; Rezende, M. C. Hygrothermal effects on dynamic mechanical analysis and fracture behavior of polymeric composites. *Materials Research* **2005**, *8*, 335-340, <https://doi.org/10.1590/S1516-14392005000300019>.
15. Chateauminois, A.; Vincent, L.B.; Chabert; Soulier, J. P. Study of the interfacial degradation of a glass-epoxy composite during hygrothermal ageing using water diffusion measurements and dynamic mechanical thermal analysis. *Polymer* **1994**, *35*, 4766-4774, [https://doi.org/10.1016/0032-3861\(94\)90730-7](https://doi.org/10.1016/0032-3861(94)90730-7).
16. Masoodi, R.; Pillai, K. M. A study on moisture absorption and swelling in bio-based jute-epoxy composites. *Journal of Reinforced Plastics and Composites* **2012**, *31*, 285-294, <https://doi.org/10.1177/0731684411434654>.
17. Leman, Z.; Sapuan, S. M.; Saifol, A. M.; Maleque, M. A.; Ahmad, M. M. H. M. Moisture absorption behavior of sugar palm fiber reinforced epoxy composites. *Materials & Design* **2008**, *29*, 1666-1670, <https://doi.org/10.1016/j.matdes.2007.11.004>.
18. Kushwaha, P. K.; Kumar, R. Studies on water absorption of bamboo-polyester composites: effect of silane treatment of mercerized bamboo. *Polymer-Plastics Technology and Engineering* **2009**, *49*(1), 45-52, <https://doi.org/10.1080/03602550903283026>.
19. Jacob, M.; Varughese, K. T.; Thomas, S. Water sorption studies of hybrid biofiber-reinforced natural rubber biocomposites. *Biomacromolecules* **2005**, *6*, 2969-2979, <https://doi.org/10.1021/bm050278p>.
20. Céline, A.; Fréour, S.; Jacquemin, F.; Casari, P. The hygroscopic behavior of plant fibers: a review. *Frontiers in Chemistry* **2014**, *1*, 43, <https://doi.org/10.3389/fchem.2013.00043>.
21. Turmanova, S.; Dimitrova, A.; Vlaev, L. Comparison of Water Absorption and Mechanical Behaviors of Polypropylene Composites Filled with Rice Husks Ash. *Polymer-Plastics Technology and Engineering* **2008**, *47*, 809-818, <https://doi.org/10.1080/03602550802188706>.

22. Deo, C.; Acharya, S. K. Effect of moisture absorption on mechanical properties of chopped natural fiber reinforced epoxy composite. *Journal of reinforced plastics and composites* **2010**, 29, 2513-2521, <https://doi.org/10.1177/0731684409353352>.
23. Munoz, E.; and , García-Manrique, J. A. Water absorption behaviour and its effect on the mechanical properties of flax fibre reinforced bioepoxy composites. *International Journal of Polymer Science* **2015**, 2015, <https://doi.org/10.1155/2015/390275>.
24. Stamboulis, A.; Baillie, C. A.; Peijs, T. Effects of environmental conditions on mechanical and physical properties of flax fibers. *Composites Part A: Applied Science and Manufacturing* **2001**, 32, 1105-1115, [https://doi.org/10.1016/S1359-835X\(01\)00032-X](https://doi.org/10.1016/S1359-835X(01)00032-X).
25. Rathinavel, S.; Saravanakumar, S. S. Development and Analysis of Poly Vinyl Alcohol/Orange peel powder biocomposite films. *Journal of Natural Fibers* **2020**, 1-10, <https://doi.org/10.1080/15440478.2019.1711285>.
26. Naik, P.; Sahoo, P.; Acharya, S. K.; Pradhan, S. Erosive wear behavior of bio-waste particulate-reinforced epoxy composites for low cost applications. *Journal of the Indian Academy of Wood Science* **2021**, 18, <https://doi.org/10.1007/s13196-020-00272-y>.
27. Naik, P.; Acharya, S. K.; Sahoo, P.; Pradhan, S. Abrasive wear behaviour of orange peel (biowaste) particulate reinforced polymer composites. *Proceedings of the Institution of Mechanical Engineers, Part J: Journal of Engineering Tribology*, **2021**, 1350650121991412, <https://doi.org/10.1177/1350650121991412>.
28. Vijay, R.; Manoharan, S.; Arjun, S.; Vinod, A.; Singaravelu, D. L. Characterization of Silane-Treated and Untreated Natural Fibers from Stem of Leucas Aspera. *Journal of Natural Fibers* **2020**, 1-17, <https://doi.org/10.1080/15440478.2019.1710651>.
29. Raghavendra, G.; Kumar, K. A.; Kumar, M. H.; Raghu Kumar, B.; Ojha, S. Moisture absorption behavior and its effect on the mechanical properties of jute-reinforced epoxy composite. *Polymer Composites* **2017**, 38, 516-522, <https://doi.org/10.1002/pc.23610>.
30. Shi, S. Q.; Gardner, D. J. Effect of density and polymer content on the hygroscopic thickness swelling rate of compression molded wood fiber/polymer composites. *Wood and Fiber Science* **2007**, 38, 520-526, <https://wfs.swst.org/index.php/wfs/article/view/15>.
31. Bera, T.; Mohanta, N.; Prakash, V.; Pradhan, S.; Acharya, S. K. Moisture absorption and thickness swelling behaviour of luffa fibre/epoxy composite. *Journal of Reinforced Plastics and Composites* **2019**, 38(19-20), 923-937, <https://doi.org/10.1177/0731684419856703>.
32. Shakeri, A.; Ghasemian, A. Water absorption and thickness swelling behavior of polypropylene reinforced with hybrid recycled newspaper and glass fiber. *Applied Composite Materials* **2010**, 17, 183-193, <https://doi.org/10.1007/s10443-009-9111-9>.
33. Jawaid, M. H. P. S.; Khalil, H. A.; Khanam, P. N.; Bakar, A. A. Hybrid composites made from oil palm empty fruit bunches/jute fibres: Water absorption, thickness swelling and density behaviours. *Journal of Polymers and the Environment* **2011**, 19, 106-109, <https://doi.org/10.1007/s10924-010-0203-2>.
34. Chaudhary, V.; Bajpai, P. K.; Maheshwari, S. Effect of moisture absorption on the mechanical performance of natural fiber reinforced woven hybrid bio-composites. *Journal of Natural Fibers* 2020, 17, 84-100, <https://doi.org/10.1080/15440478.2018.1469451>.
35. M. Haameem, J. A.; Abdul Majid, M. S.; Afendi, M.; Marzuki, H. F. A.; Hilmi, E. A.; Fahmi, I.; Gibson, A. G. Effects of water absorption on Napier grass fibre/polyester composites. *Composite Structures* **2016**, 144, 138-146, <https://doi.org/10.1016/j.compstruct.2016.02.067>.
36. Patel, B. C.; Acharya, S. K.; Mishra, D. Environmental effect of water absorption and flexural strength of red mud filled jute fiber/polymer composite. *International Journal of Engineering, Science and Technology* **2012**, 4, 49-59, <https://doi.org/10.4314/ijest.v4i4.4>.
37. Sinha, A. K.; Narang, H. K.; Bhattacharya, S. Mechanical properties of natural fibre polymer composites. *Journal of Polymer Engineering* **2017**, 37, 879-895, <https://doi.org/10.1515/polyeng-2016-0362>.
38. Elanchezhian, C.; Ramnath, B. V.; Ramakrishnan, G.; Rajendrakumar, M.; Naveenkumar, V.; Saravanakumar, M. K. Review on mechanical properties of natural fiber composites. *Materials Today: Proceedings* **2018**, 5, 1785-1790, <https://doi.org/10.1016/j.matpr.2017.11.276>.
39. Alomayri, T.; Assaedi, H.; Shaikh, F. U. A.; Low, I. M. Effect of water absorption on the mechanical properties of cotton fabric-reinforced geopolymer composites. *Journal of Asian ceramic societies* **2014**, 2, 223-230, <https://doi.org/10.1016/j.jascer.2014.05.005>.
40. Gobikannan, T.; Berihun, H.; Aklilu, E.; Pawar, S. J.; Akele, G.; Agazie, T.; Bihonegn, S. Development and Characterization of Sisal Fiber and Wood Dust-Reinforced Polymeric Composites. *Journal of Natural Fibers* **2020**, 1-10, <https://doi.org/10.1080/15440478.2019.1710649>.

41. Banerjee, S.; Sarkar, P.; & Sahoo, P. Improving corrosion resistance of magnesium nanocomposites by using electroless nickel coatings. *Facta Universitatis, Series: Mechanical Engineering*, **2021**, <http://casopisi.junis.ni.ac.rs/index.php/FUMechEng/article/view/7833>.
42. Mukhopadhyay, A.; & Sahoo, S. A Grey-Fuzzy based approach for the optimization of corrosion resistance of rebars coated with ternary electroless nickel coatings. *Journal of Soft Computing in Civil Engineering* **2022**, *6*, 107-127, <https://dx.doi.org/10.22115/scce.2022.326903.1401>.
43. Mukhopadhyay, A.; & Sahoo, S. Optimized electroless Ni-Cu-P coatings for corrosion protection of steel rebars from pitting attack of chlorides. *Engineering Transactions*, **2021**, *69*, 315-332, <https://entra.put.poznan.pl/index.php/et/article/viewFile/1367/903>.
44. Mukhopadhyay, A.; & Sahoo, S. Improving corrosion resistance of reinforcement steel rebars exposed to sulphate attack by the use of electroless nickel coatings. *European Journal of Environmental and Civil Engineering*, **2021**, 1-16, <https://www.tandfonline.com/doi/abs/10.1080/19648189.2021.1886177>.
45. Mukhopadhyay, A.; & Sahoo, S. Corrosion Performance of Steel Rebars by Application of Electroless Ni-P-W Coating-An Optimization Approach using Grey Relational Analysis, *FME Transactions*, **2021**, *49*, 445-455, <https://scindeks.ceon.rs/article.aspx?artid=1451-20922102445M>.
46. Biswas, P.; Das, S. K.; & Sahoo, P. Duplex electroless Ni-P/Ni-P-W coatings: Effect of heat treatment on tribological and corrosion performance, *Materials Today: Proceedings* **2022**, <https://doi.org/10.1016/j.matpr.2022.06.042>.
47. Naik, P.; Pradhan, S.; Acharya, S. K.; & Sahoo, P. Effect of Pretreatment on the Mechanical Properties of Orange Peel Particulate (Bio-Waste)-Reinforced Epoxy Composites. *International Journal of Manufacturing, Materials, and Mechanical Engineering (IJMMME)* **2022**, *12*, 1-25, <http://doi.org/10.4018/IJMMME.293223>.
48. Naik, P.; Pradhan, S.; Acharya, S. K.; & Sahoo, P. Effect of Carbonization of Orange Peel Particulate-Reinforced Polymer Composites: Mechanical and Morphological Properties. *International Journal of Surface Engineering and Interdisciplinary Materials Science (IJSEIMS)*, **2022**, *10*, 1-20, <http://doi.org/10.4018/IJSEIMS.295097>.
49. Jena, H.; Panigrahi, A.; & Jena, M. Mechanical property of jute fibre reinforced polymer composite filled with clam shell filler: a marine waste, *Advances in Materials and Processing Technologies*, **2022**, 1-17, <https://doi.org/10.1080/2374068X.2022.2085387>.
50. Owuamanam, S.; Soleimani, M.; Cree, D.E. Fabrication and Characterization of Bio-Epoxy Eggshell Composites. *Appl. Mech.* **2021**, *2*, 694–713. <https://doi.org/10.3390/applmech2040040>
51. Khan, M. W.; Elayaperumal, A.; Prabhu, M. S.; & Arulvel, S. Effect of compaction pressure on the physical, mechanical, and tribological behavior of compacted crab shell particles prepared using uniaxial compaction route. *Journal of Materials Engineering and Performance*, **2022**, *31*, 3493-3507, <https://link.springer.com/article/10.1007/s11665-021-06487-5>.